INTERNATIONAL JOURNAL FOR NUMERICAL METHODS IN FLUIDS, VOL. 1, 347–364 (1981)

OLD AND NEW FINITE ELEMENTS FOR INCOMPRESSIBLE FLOWS*

MICHEL FORTIN

Université Laval, Département de Mathématiques, G1K 7P4, Québec, Canada

SUMMARY

This paper presents some seemingly new elements for the computation of two and three-dimensional incompressible flow. We want to obtain elements satisfying the Babŭska–Brezzi condition for mixed methods and thus introducing no spurious pressure modes (cf. Sani *et al.*[1]). In order to present clearly the advantages and disadvantages of our new elements we compare them on a qualitative basis with more standard ones. Of particular importance for incompressible flow is the size and shape of vortices that can be produced by the elements. We shall try to describe this as precisely as possible. The conclusion is that the elements introduced here should be quite competitive on a cost/precision scale.

KEY WORDS Incompressible Flows Pressure Modes Vortices Finite Element

INTRODUCTION

Although the approximation of incompressible materials is not a new field it is certainly true that it is still a rapidly evolving subject. There has been, for a long time, a wide gap between theoretical results and practice. Computations were done, with success, using theoretically dubious elements or at best using elements for which theory was silent. On the other hand, elements for which convergence proofs were available were treated with suspicion by code developers.

In the past few years, however, it has become more and more evident that in order to obtain a reliable numerical code, one needs some understanding of the convergence properties of the elements used. In particular, penalty methods have been shown to work if and only if the associated mixed method works. (The reader may refer to Malkus and Hugues.[2]) One is then brought back to studying the convergence of mixed, velocity–pressure, approximations and thus to the Babŭska–Brezzi compatibility condition for mixed methods: one cannot mix together *any* approximation of velocity with *any* approximation of pressure.

The main idea has nothing to do with any particular physical problem, it is strictly related to the approximation of a divergence-free vector field. To fix ideas we shall consider a simple model problem: Stokes flow in a bounded domain Ω of $\mathbb{R}^n$ ($n = 2$ or 3). We define on Ω,

$$L^2(\Omega) = \left\{ u \;\middle|\; \int_\Omega |u(x)|^2 \, dx \right\}, \tag{1}$$

the space of square integrable functions and

$$H_0^1(\Omega) = \{ u \mid u \in L^2(\Omega),\ \nabla u \in (L^2(\Omega))^n,\ u|_{\partial\Omega} = 0 \}. \tag{2}$$

* This work was partly supported by NSERC Grant 8195 and a 'subvention FCAC' from the Ministère de l'éducation du Québec.

0271–2091/81/040347–18$01.80

Received 20 March 1981
Revised 29 June 1981

and also

$$V = (H_0^1(\Omega))^n \tag{3}$$

The space V contains vector fields vanishing on the boundary of Ω.

We now look for $\mathbf{u} \in V$ and $p \in L^2(\Omega)$ such that for a given $\mathbf{f} \in L^2(\Omega)$

$$\left.\begin{aligned} -\Delta \mathbf{u} + \nabla \mathbf{p} &= \mathbf{f} \\ \nabla \cdot \mathbf{u} &= 0 \\ \mathbf{u}|_{\partial\Omega} &= 0 \end{aligned}\right\} \tag{4}$$

or in an equivalent variational formulation

$$\sum_{i=1}^{n} \int_\Omega \frac{\partial u_i}{\partial x_i} \frac{\partial v_i}{\partial x_i} \, dx - \int_\Omega p \nabla \cdot \mathbf{v} \, dx = \int_\Omega \mathbf{f} \cdot \mathbf{v} \, dx \qquad \forall \mathbf{v} \in V \tag{5}$$

$$\int_\Omega \nabla \cdot \mathbf{u} q \, dx = 0, \qquad \forall q \in L^2(\Omega). \tag{6}$$

Let us now suppose that V_h and Q_h are finite element approximations of V and $L^2(\Omega)$ respectively. We can solve in $V_h \times Q_h$ the discrete analogue of (5), (6). Let us try to see more clearly the meaning of this discrete problem, particularly of the discrete form of (6) which can be written

$$\int_\Omega \nabla \cdot \mathbf{u}_h q_h \, dx = 0, \qquad \forall q_h \in Q_h. \tag{7}$$

This means that the *projection* in an $L^2(\Omega)$ norm of $\nabla \cdot \mathbf{u}_h$ on Q_h is zero. In general this is a weaker condition than $\nabla \cdot \mathbf{u}_h = 0$. Let us take as an example Q_h built from piece-wise constant functions. Then (7) means that on any element K, one has

$$\int_K \nabla \cdot \mathbf{u}_h \, dx = \int_{\partial K} \mathbf{u}_h \cdot \mathbf{n} \, d\sigma = 0. \tag{8}$$

This expresses the balance of mass on K and it is indeed an intuitively correct approximation to $\nabla \cdot \mathbf{u}_h = 0$.

To be more precise (7) defines a *discrete divergence operator* from V_h into Q_h and we shall denote this operator by B_h. It is defined by:

$$\left.\begin{aligned} & B_h \mathbf{u}_h \in Q_h \\ & \int_\Omega (B_h \mathbf{u}_h) q_h \, dx = \int_\Omega \nabla \cdot \mathbf{u}_h q_h \, dx, \qquad \forall q_h \in Q_h. \end{aligned}\right\} \tag{9}$$

The transposed operator $B_h^T (\int_\Omega B_h \mathbf{u}_h q_h \, dx = \int_\Omega u_h \cdot B_h^T q_h \, dx)$ is the discrete analogue of $-\nabla$, the gradient operator.

Let us now define the *subspace* of discrete-divergence-free vector fields.

$$Z_h = \left\{ \mathbf{u}_h \;\middle|\; B_h \mathbf{u}_h = 0 \quad \text{or} \quad \int_\Omega \nabla \cdot \mathbf{u}_h q_h \, dx = 0 \quad \forall q_h \right\}. \tag{10}$$

The *first question* that arises is whether or not $B_h^T p_h = 0$ implies $p_h =$ constant which is the discrete analogue of the fact that $\nabla p = 0$ implies $p =$ constant. The former is not always true. If the kernel of B_h^T is more than one-dimensional our approximation will contain *spurious pressure modes*. If no spurious modes can occur it is fairly easy to obtain the error estimate

(see Temam[3] or Girault and Raviart[4] for instance).

$$\|\mathbf{u}-\mathbf{u}_h\|_V + \|p-p_h\|_{L^2(\Omega)/\mathbb{R}} \leq c_1 \inf_{\mathbf{v}_h \in Z_h} \|\mathbf{u}-\mathbf{v}_h\|_V + c_2 \inf_{q_h \in Q_h} \|p-q_h\|_{L^2(\Omega)/\mathbb{R}}. \tag{11}$$

where

$$\|q\|_{L^2(\Omega)/\mathbb{R}} = \inf_{c \in \mathbb{R}} \|q+c\|_{L^2(\Omega)}$$

is a quotient norm and must be used because p is defined up to an additive constant. In order to be able to use (11) one would like to have

$$\inf_{\mathbf{v}_h \in Z_h} \|\mathbf{u}-\mathbf{v}_h\|_V \leq c_3 \inf_{\mathbf{v}_h \in V_h} \|\mathbf{u}-\mathbf{v}_h\|; \tag{12}$$

that is, discrete-divergence-free vector fields approximate divergence-free vector fields at optimal order. This is the *second question* that must be answered.

It turns out that the answer to both questions is contained in the Babŭska–Brezzi condition: there must exist a constant k independent of h such that

$$\sup_{\mathbf{v}_h \in V_h} \frac{\int_\Omega p_h \nabla \cdot \mathbf{v}_h \, dx}{\|v_h\|_V} \geq k \|p_h\|_{L^2(\Omega)/\mathbb{R}}. \tag{13}$$

This condition is, however, rather abstract and is generally hard to check directly. It was however shown in Fortin[5] and was implicitly used in Crouzeix and Raviart[6] and Fortin[7] that checking (13) can in some cases be recast as an 'interpolation' problem. Condition (13) was introduced by Brezzi[8] and in another form by Babŭska.[9]

Precisely, (13) will be satisfied whenever, given a vector field $\mathbf{u} \in V$, one can explicitly build (that is, one can describe a way to do so) a discrete vector field $\mathbf{u}_h$ such that

$$\int_\Omega \nabla \cdot \mathbf{u}_h q_h \, dx = \int_\Omega \nabla \cdot \mathbf{u} q_h \, dx \qquad \forall q_h \in Q_h, \tag{14}$$

or $B_h \mathbf{u}_h = B_h \mathbf{u}$, and such that $\mathbf{u}_h$ depends continuously on $\mathbf{u}$.

For instance if Q_h is built from piece-wise constant functions, that means building an 'interpolate' $\mathbf{u}_h$ such that

$$\int_K \nabla \cdot \mathbf{u}_h \, dx = \int_K \nabla \cdot \mathbf{u} \, dx$$

for any element K, that is $\mathbf{u}_h$ has the same balance of mass as $\mathbf{u}$ on every element. The following developments intend to describe elements for which this can be done. We shall then be sure that these approximations will be free of spurious pressure modes and be able to use the error estimate (12).

To complete this introduction, we need to describe the basic structure of an incompressible vector field. This is quite simple for two-dimensional fields but far more intricate for three-dimensional ones. We only consider fields vanishing outside a bounded domain which we take to be simply connected (without holes) for simplicity. The basic structure of a divergence-free field is the vortex: we mean by this a recirculating flow circling around a centre. We do not elucidate the real structure of a vortex for we only want to obtain an approximate image. We represent a vortex by a circle, with the direction of rotation shown by

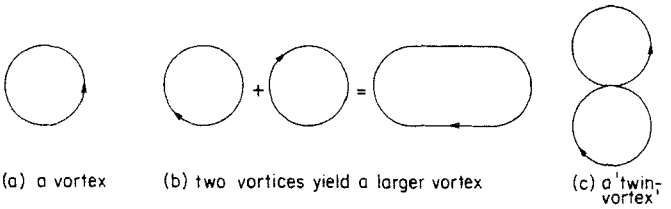

Figure 1

an arrow. Vortices combine to form larger vortices or more complex structures. In particular we shall quite often meet the 'twin-vortex' of Figure 1(c). The size of the smallest representable vortex is the equivalent for incompressible flows of the largest frequency in spectral methods.

For three-dimensional fields, the basic structure is still the 'flat vortex' of the two-dimensional case. But it can now take any orientation in space and very complex structures can now be built. A very simple one is the 'roll'. It can be obtained by piling flat vortices (Figure 2).

Figure 2. The roll

The roll is essentially a two-dimensional structure. Closing a roll on itself we obtain what could be called a doughnut (Figure 3). This torus-like structure is the three-dimensional analogue of the twin vortex.

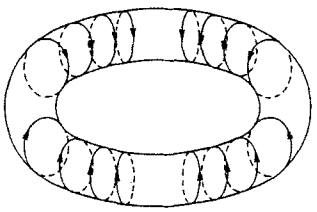

Figure 3. The doughnut

Finally piling doughnuts would yield what we could call tubes. A regular array of doughnuts (or tubes) would yield something very similar to the hexagonal convection cells of Bénard. When describing three-dimensional elements we shall try to exhibit, at least, the rolls and doughnuts they can produce.

TWO-DIMENSIONAL INCOMPRESSIBLE ELEMENTS

We want to introduce here a new quadrilateral element for incompressible flow. The reasons for introducing it can, however, be made clear only if we relate it to more standard elements. The idea is to look for the simplest element for which the Babŭska–Brezzi condition can be checked and thus be free of spurious pressure modes. We shall therefore review many

standard elements with respect to the Babuska–Brezzi (B.B.) condition and convergence order and also in a less standard way with respect to the size of the smallest representable vortices for a given mesh. We think that the latter is a more reliable and intuitive point of view for incompressible flow problems. We refer the reader to the related work of Griffiths[10,11] where a similar idea is developed but for a different purpose: divergence-free bases are built for computational purposes.

We first need to give some definitions. A quadrilateral isoparametric element is defined by its image on a reference rectangle $\hat{K}$ on which co-ordinates are $\hat{x}$ and $\hat{y}$. We assume the reader to be familiar with this technique and we shall restrict most of our presentation to $\hat{K} = [-1, 1] \times [-1, 1]$, the unit square.

We denote by P_k the set of polynomials of degree k on $\hat{K}$ and by Q_k the set of functions that are polynomials of degree k in each co-ordinate, the other one being fixed. In particular functions of Q_k are polynomials of degree k on the boundary of $\hat{K}$. We say that functions of Q_1 are bilinear functions. They are normally defined by their values at the four vertices. The latter ensures interelement continuity. We distinguish between $Q_2^{(8)}$ and $Q_2^{(9)}$, respectively the 8-node and 9-node biquadratic elements. (See for instance Strang and Fix[12] or any introduction to finite elements.) We shall say that functions of $Q_2^{(8)}$ are biquadratic and those of $Q_2^{(9)}$ full biquadratic.

We can now present our first example.

Example 1: *The $Q_1 - P_0$, bilinear velocity–constant pressure, element*

This is a widely used and well-known element. The degrees of freedom are the values of u_1 and u_2 at the corners of K and a constant value of pressure that can be associated if desired with the barycentre M_0 of the element (Figure 4).

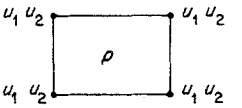

Figure 4

The discrete-divergence-free condition is therefore a mass–balance condition on every element. That means a linear constraint between the nodal values of $\mathbf{u}_h$ for each element. These conditions are not all linearly independent: indeed we have

$$\sum_K \int_K \nabla \cdot \mathbf{u}_h \, dx = \int_\Omega \nabla \cdot \mathbf{u}_h \, dx = \int_{\partial\Omega} \mathbf{u}_h \cdot \mathbf{n} \, d\sigma = 0 \tag{15}$$

i.e. the sum of the constraints is zero. This is equivalent to saying that B_h^T has constant functions in its kernel. In some cases, however, there is more than one linear relation between constraints.

This element is in fact well-known to suffer from a checkerboard pressure mode[1] on regular meshes: the approximate pressures are defined up to *two* additive constants, each one acting on respectively the red and black squares of the checkerboard. The existence of this spurious pressure mode implies that this element does not satisfy the B. B. condition. It is quite easy to exhibit the shape and size of representable vortices using this element on a regular $n \times n$ mesh. We have $2(n-1)^2$ degrees of freedom (u_1 and u_2 at interior modes), linked by $n^2 - 2$ independent linear constraints. This leaves $(n-2)^2$ independent vortices. The smallest one

covers a 3×3 array and it is easy to see that all $(n-2)^2$ vortices are generated by linear combinations of such 3×3 vortices. This elementary vortex is sketched on Figure 5: in this figure as in the subsequent ones we represent by arrows the value of the vector field at the nodes of the element.

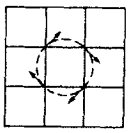

Figure 5. The smallest vortex for (Q_1-P_0) elements

Example 2: 8-node biquadratic velocity–constant pressure element $(Q_2^{(8)}-P_0)$

This is still a well-known element. If we refer to error estimate (12) it is seen that we have here a poor element: the approximation of pressure is only first order while the approximation of velocity can be second order. We shall also see later that there is no computational reason to use this element as a similar element *can be made second order without increasing the number of degrees of freedom.*

However, we believe it is worth presenting a complete analysis and relating this element to its analogues. The degrees of freedom of the element are presented in Figure 6.

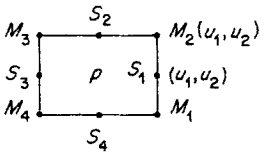

Figure 6. The $Q_2^{(8)}-P_0$ element

We number M_1, M_2, M_3, M_4 the vertices of the element and S_1, S_2, S_3, S_4 its sides. The nodes are at the vertices and mid-side points and to each node we associate the two components of velocity u_1, u_2. The constant value p of pressure can be associated to the barycentre M_0 of the element.

This element is easily seen to satisfy the B.B. condition. The simplest way to do so is to build explicitly an interpolation operator preserving discrete divergence. The discrete-divergence-free condition is again a mass–balance condition on every element. Let

$$\mathbf{u}=\{u_1, u_2\}$$

be a given vector field. We define its interpolate by setting on each element K

$$u_{jh}(M_i)=u_j(M_i) \qquad i=1,2,3,4 \tag{16a}$$

$$\int_{S_i} u_{jh}\,d\sigma=\int_{S_i} u_j\,d\sigma \qquad i=1,2,3,4 \tag{16b}$$

for both components u_{1h} and u_{2h} of $\mathbf{u}_h$. Condition (16b) can be satisfied because of the presence of the velocity at mid-side points as a degree of freedom. Condition (16b) implies that

$$\int_{\partial K} \mathbf{u}_h\cdot\mathbf{n}\,d\sigma=\int_{\partial K}\mathbf{u}\cdot\mathbf{n}\,d\sigma$$

and thus that the discrete-divergence-free condition is preserved by the choice of $\mathbf{u}_h$. It is fairly easy to check by the methods of Crouzeix-Raviart[6] that $\mathbf{u}_h$ approximates $\mathbf{u}$ with optimal order. This property indirectly proves the B.B. condition according to the result of Fortin.[5]

The *secret of this success* is the presence of a mid-side velocity node which permits control of the flow across the boundary of the element.

Let us now consider the size and shape of vortices for a regular mesh of $n \times n$ such elements. We have

$$2(n-1)^2+4n(n-1)$$

degrees of freedom linked by n^2-1 (no spurious mode) linear constraints. This leaves

$$3(n-1)^2+2n(n-1)$$

degrees of freedom or independent vortices. The last $2n(n-1)$ of these can, however, be considered as *spurious vortices* as they do not correspond to a recirculating flow. We sketch the seven existing vortices for $n=2$ on Figure 7.

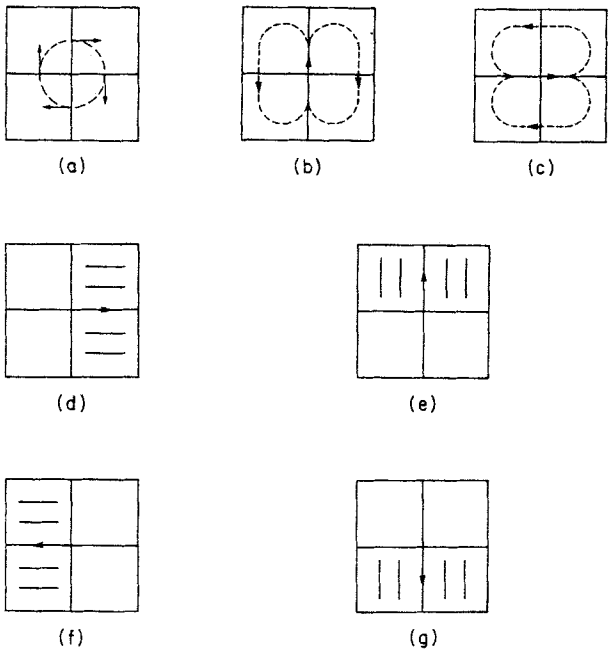

Figure 7. The smallest vortices for $Q_2^{(8)}-P_0$ element

The last four are spurious in the sense that a flow parallel to a side does not violate the mass balance in elements but is not qualitativley vortex-like. The cure for this lies in the next elements considered.

Example 3: *9-node (full) biquadratic velocity–linear pressure element* ($Q_2^{(9)} - P_1$)

The element we now consider is probably the best one known for two-dimensional incompressible computations. It is second-order accurate and can be reduced to the same number of degrees of freedom as the previous one. We use the same labelling of nodes as in Figure 6. We now, however, use a full biquadratic approximation for velocity and we associate two degrees of freedom u_1, u_2 with the barycentre M_0. Pressure is now a linear ($p = a_0 + a_1 x + a_2 y$) function.

We shall again prove that this element satisfies the B.B. condition by explicitly building an interpolate for a divergence-free vector field $\mathbf{u}$. But first let us consider in more detail the discrete-divergence-free condition. We now require that on any element K

$$\int_K \nabla \cdot \mathbf{u}_h p_h \, dx = 0, \quad \forall p_h \quad \text{linear function of } x \text{ and } y. \tag{17}$$

This can be decomposed into three conditions

$$\text{(a)} \int_K \nabla \cdot \mathbf{u}_h \, dx = 0, \qquad \text{(b)} \int_K \nabla \cdot \mathbf{u}_h (x - \bar{x}) \, dx = 0$$
$$\text{(c)} \int_K \nabla \cdot \mathbf{u}_h (y - \bar{y}) \, dx = 0 \tag{18}$$

where $\bar{x}$ and $\bar{y}$ are the co-ordinates of the barycentre M_0 of K. But the last two [(b) and (c)] of these conditions are linear relations between the values of u_1, u_2 on the boundary of K and the values at M_0. Indeed we have, for instance,

$$\int_K \nabla \cdot \mathbf{u}_h (x - \bar{x}) \, dx = -\int_K u_{1h} \, dx + \int_{\partial K} \mathbf{u}_h \cdot \mathbf{n} (x - \bar{x}) \, d\sigma. \tag{19}$$

But all these integrals can be computed by Simpson's rule (on the reference rectangle) and depend linearly on the nodal values. This means that the degrees of freedom u_1, u_2 at M_0 can be linked (as in standard serendipity elements) to the degrees of freedom at the boundary. We are therefore *computationally* left with an 8-node, constant pressure element. Verifying the B.B. condition can now be done with the same interpolate (16) as we used in the previous example, provided the values of $\mathbf{u}$ at M_0 are defined through (18b) and (18c).

With respect to the size, number, and shape of independent vortices we have the same count, $3(n-1)^2 + 2n(n-1)$ independent vortices on an $n \times n$ mesh. But here none are spurious. For instance the vortex equivalent to Figure 7(d) is now sketched in Figure 8.

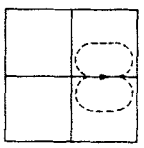

Figure 8

It is now a genuine vortex since the values of u_1 and u_2 at M_0, although linked to other nodes, allow recirculation *inside* an element. It is interesting to note that this vortex is now a smaller copy of the twin-vortices (b) of Figure 7.

Example 4: Restricted 8-node biquadratic–constant pressure element

This example introduces a 'new' element and in fact the simplest one for which one can prove the B.B. condition. The reasons for introducing it are not very strong for two-dimensional problems but the extension to 3-D cases is surely important.

If we refer to the way we have verified the B.B. condition for the two previous elements it is clear that a crucial point was the presence of mid-side nodes enabling us to control

$$\int_S \mathbf{u}_h \cdot \mathbf{n} \, d\sigma$$

on a given side S. However, we also had a control on the tangential component

$$\int_S \mathbf{u}_h \cdot \mathbf{t} \, d\sigma$$

but did not use it. The idea is now to suppress this last degree of freedom and to retain only the normal component of velocity at mid-side nodes. We also want this element to tolerate Q_1 deformations, or equivalently we want to be able to use any quadrilateral element with straight sides. The degrees of freedom of this element are presented in Figure 9.

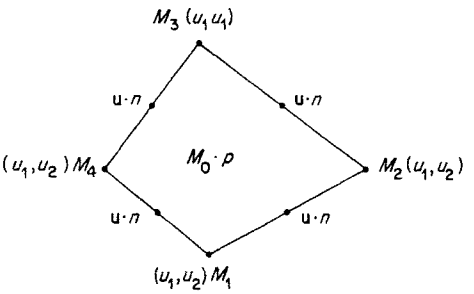

Figure 9

The only real new feature is the construction of such an element from standard techniques, that is using a reference element. It is easy to build shape functions on $\hat{K}$ satisfying our definition of the element, but they *cannot* be used as reference shape functions because the normal component does not remain the normal component when passing from $\hat{K}$ to K. However, the cure is in fact very simple.

Let $\hat{K}$ be a reference rectangle and

$$F(\hat{x}) = \{F_1(\hat{x}_1, \hat{x}_2), F_2(\hat{x}_1, \hat{x}_2)\}$$

be the Q_1 transformation mapping $\hat{K}$ on K. If $\hat{u}(\hat{x})$ is defined on $\hat{K}$, we set on K, $\mathbf{u}(x) = \hat{\mathbf{u}}(F^{-1}(x))$. We now want to define $\hat{\mathbf{u}}$ on K such that $\mathbf{u}$ will satisfy on any side S of K the following conditions

$\mathbf{u} \cdot \mathbf{t}$, the tangential component of $\mathbf{u}$ is linear on S. (20a)

$\mathbf{u} \cdot \mathbf{n}$, the normal component of $\mathbf{u}$ is a quadratic polynomial on S. (20b)

The easiest way to do so is to separate $\mathbf{u}$ and $\hat{\mathbf{u}}$ into a bilinear part and a biquadratic correction:

$$\mathbf{u} = \hat{\mathbf{u}}_1(F^{-1}(x)) + \hat{\mathbf{u}}_2(F^{-1}(x)) = \mathbf{u}_1 + \mathbf{u}_2 \tag{21}$$

where $\hat{\mathbf{u}}_1 \in Q_1$, $\hat{\mathbf{u}}_2 \in Q_2^{(8)}$. The first part $\mathbf{u}_1$ is a standard Q_1 and both of its components (tangential and normal) are linear on the sides of K.

The second component $\hat{\mathbf{u}}_2$ is defined as follows:

Let $\hat{S}_i$ be the side of $\hat{K}$ corresponding to the side S_i of K; we denote by $\hat{N}_i$ the mid-side point of $\hat{S}_i$ and by N_i the mid-side point of S_i. Let also

$$\mathbf{n}(x) = \{n_1(x), n_2(x)\}$$

be the unit normal to ∂K at point $x \in \partial K$. It will be necessary to choose an orientation of $\mathbf{n}(x)$ that is the same in adjacent elements: one could for instance take $n_1(x)$ to be positive and $n_2(x)$ to be positive if $n_1(x)$ vanishes.

We now define on side $\hat{S}_i$ a shape function $\mathbf{p}_i(\hat{x})$ by setting

$$\mathbf{p}_i(\hat{x}) \in Q_2^{(8)} \times Q_2^{(8)} \tag{22a}$$

$$\mathbf{p}_i(\hat{x}) = 0 \quad \text{on} \quad S_j, \qquad j \neq i \tag{22b}$$

$$\mathbf{p}_i(\hat{N}_i) = \mathbf{n}(N_i) \tag{22c}$$

Condition (22b) implies in particular that $\mathbf{p}_i(\hat{x})$ vanishes at the four corners of $\hat{K}$.

Condition (22c) makes $\mathbf{p}_i(\hat{x})$ depend on the geometry of K in a very simple (linear) way. Setting now

$$\mathbf{u}_2(x) = \sum_{i=1}^{4} c_i \mathbf{p}_i(P^{-1}(x)) \tag{23}$$

it is easy to check that $\mathbf{u}_2 \cdot \mathbf{t}$ is everywhere zero on ∂K and that

$$\mathbf{u}_2 \cdot \mathbf{n} = c_i \quad \text{at} \quad N_i. \tag{24}$$

The tangential component of $\mathbf{u} = \mathbf{u}_1 + \mathbf{u}_2$ thus remains linear while the normal component is quadratic.

This completes the description of the element which we denote $R_2^{(8)} - P_0$ for 'restricted biquadratic velocity'–constant pressure element. It is easy to check the B.B. condition using an interpolate similar to (16).

With respect to the shape of vortices on an $n \times n$ mesh, we have $2(n-1)^2 + 2n(n-1)$ degrees of freedom linked by $n^2 - 1$ linear constraints. This leaves $3(n-1)^2$ independent vortices. On a 2×2 mesh these three vortices are exactly (a), (b) and (c) of Figure 7. The elimination of the tangential velocity node at mid-side points has eliminated the four spurious vortices (d), (e), (f) and (g). □

To end this section, we shall try to summarize our results in order to compare the previously described elements. Table I presents the main results concerning these elements on an $n \times n$ mesh.

The first obvious remark is that $Q_2^{(8)} - P_0$ should never be used. It can be made second order (and spurious vortices can be made genuine) at no extra cost. The alternative is to eliminate spurious vortices by using $R_2^{(8)} - P_0$. The real question is then whether or not one should use the 'simple' element $Q_1 - P_0$ or $R_2^{(8)} - P_0$ if one is happy with a first-order approximation. We claim that it is *essentially no more expensive* to use $R_2^{(8)} - P_0$ which is a more reliable element, satisfying the B.B. condition. To see this let n be the mesh size for a

Table I

Element	Approximate number of d.o.f.	Approximate number of independent vortices	Order of convergence	Remarks
Q_1-P_0	$2n^2$	n^2	First	Checkerboard pressure mode
$Q_2^{(8)}-P_0$	$6n^2$	$5n^2$	First	Spurious (non-recirculating) 'vortices'
$Q_2^{(9)}-P_1$	$6n^2$	$5n^2$	Second	Internal nodes are eliminated at element level
$R_2^{(8)}-P_0$	$4n^2$	$3n^2$	First	No spurious pressure modes or vortices

Q_1-P_0 discretization and $\hat{n}$ the mesh size for a $R_2^{(8)}-P_0$ approximation. But Q_1-P_0 yields n^2 vortices while $R_2^{(8)}-P_0$ yields $3\hat{n}^2$. We could then use $\hat{n}^2=\frac{1}{3}n^2$, and $4\hat{n}^2=\frac{4}{3}n^2$ degrees of freedom instead of $2n^2$ for Q_1-P_0.

But this simple count is probably much too optimistic. On a more secure ground, let us just consider the fact that the smallest vortex of $R_2^{(8)}-P_0$ needs a 2×2 array [Figure 7(a)] while it needs a 3×3 array for Q_1-P_0 (Figure 5.) On the basis of the smallest representable vortex we could therefore use $\hat{n}=\frac{2}{3}n$ or $4\hat{n}^2=\frac{16}{9}n^2$ instead of $2n^2$ degrees of freedom. Of course other facts should be taken into account, for instance band-width in the linear problems. However, we believe that $R_2^{(8)}-P_0$ is a reliable element, free from spurious features and very competitive on a precision/cost scale. We shall now try to extend it to the three-dimensional case.

THREE-DIMENSIONAL INCOMPRESSIBLE ELEMENTS

We now want to consider some three-dimensional analogues of the elements described in the previous section. As we shall see, these analogues are not always straightforward and some adjustments will have to be made. We again want to know which elements satisfy the B.B. condition and again we shall try to check this by explicitly building an interpolation operator preserving the mass balance condition on elements. The main remark concerning this condition is that we now have to consider the flow through the faces of a cube (or in general a hexahedron) and that edges are now irrelevant. We shall again try to present the elementary vortices for the elements considered. This is much more difficult than in the two-dimensional case. We apologize from the start for the imperfections of our representations; we believe that they can give the interested reader the initial hint to develop his own personal insight.

We begin our analysis by presenting standard examples. In all cases we shall restrict ourselves to cubic elements and regular meshes.

Example 5: *Trilinear velocity–constant pressure element* (Q_1-P_0)

We consider on the reference cube a velocity–pressure element where each component of the velocity is a linear function of each co-ordinate, the others being fixed. This is a direct analogue of the Q_1-P_0 element of Example 1.

The element is presented in Figure 10.

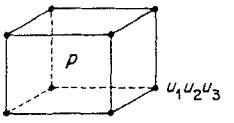

Figure 10

The degrees of freedom are the values u_1, u_2, u_3 of velocity at the vertices of the cube and a constant value of pressure on each element. This is the simplest possible hexahedral element and this is probably the only reason why it is used. Before discussing the properties of this element, we shall exhibit the mass balance condition that corresponds here to the discrete-divergence-free condition. We must have for any element K

$$\int_K \nabla \cdot \mathbf{u}_h \, dx = 0 = \int_{\partial K} \mathbf{u}_h \cdot \mathbf{n} \, d\sigma = \sum_{i=1}^{6} \int_{F_i} \mathbf{u}_h \cdot \mathbf{n} \, d\sigma \tag{25}$$

where $F_1, F_2, \ldots, F_6$ are the six faces of the elements.

If we want to build an interpolation operator analogous to (16) we shall have to control the flow through each face and this will be possible if and only if the normal component of $\mathbf{u}_h$ is an explicit degree of freedom of the face. This is not the case for this element. Indeed this element is known to suffer from $3n-2$ spurious pressure modes (Sani *et al.*[1]) (on a regular mesh). That means pressure is defined up to $3n-1$ constants and that this element does not satisfy the B.B. condition. This also means that this element is restricted to regular meshes: on general meshes we may have 'impure spurious modes' in the terminology of Sani *et al.*,[1] and thus a potential instability.

As to the shape and size of vortices, let us consider an n^3 array of cubes and a field vanishing at the boundary of this array. *There are* $(n-1)^3$ *interior vertices,* $3(n-1)^2n$ *edges and* $3n^2(n-1)$ *faces.*

We thus have $3(n-1)^3$ degrees of freedom linked by n^3-3n+1 linearly independent constraints. We use the fact that there exists $3n-2$ spurious pressure modes. This leaves $3(n-2)^2(n-1)-(n-2)^3$ linearly independent vortices. We have written this result in a seemingly strange way that is in fact related to the following analysis. To illustrate these vortices, let us consider a $3\times3\times3$ array where five independent vortices should exist. Indeed they are readily found. Consider a $2\times3\times3$ sub-array and define the values of the velocity in the mid-plane P so that they correspond to the two-dimensional vortex of Figure 11.

We thus get a two-element thick three-dimensional version of this vortex. On an $n\times n\times n$ mesh there are $3(n-3)^2(n-1)$ such vortices. However, they are not all linearly independent. In our $3\times3\times3$ array we have six such vortices but only five of them are independent. It can easily be checked that the sum of any five of them yields the sixth one. This linear dependence is expressed by the last two terms of the above formula.

The elementary vortices we have identified can pile to yield $3\times3\times k$ rolls. To get a doughnut we need at least a $4\times4\times3$ array and the result is somewhat crude.

We may conclude that this element will not be adequate to compute complex flows unless the mesh size is small. We shall now try to see what can be obtained from more sophisticated elements.

Example 6: Triquadratic velocity–constant pressure element $(Q_2^{(20)}-P_0)$

In this example again, the elements used to discretize the system are classical: we use the 20-node incomplete triquadratic. The degrees of freedom are the values of velocity at the vertices and at mid-edge points of the element (Figure 12).

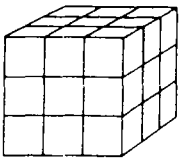

(a) The 3×3×3 array

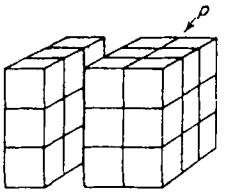

(b) The 2×3×3 sub-array

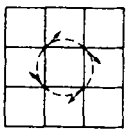

(c) The mid-plane vortex

Figure 11

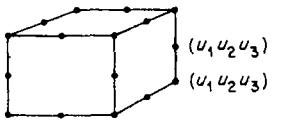

Figure 12. The $Q_2^{(20)} - P_0$ element

As we use a piece-wise constant approximation for pressure we only have a first-order accurate element and we do not use fully the accuracy of our velocity approximation. This element is the natural analogue of the two-dimensional $Q_2^{(8)} - P_o$ element. There is, however, a very important difference: the 3-D element does not satisfy the B.B. condition: a simple check on the mass balance constraints shows that *two* of them are linearly dependent on the others and that there is a *three-dimensional checkerboard* pressure mode. Anyhow, this is better than the seven spurious pressure modes of the previous element. The presence of a C.B. pressure mode must be related to the lack of a degree of freedom at mid-face points, which would enable us to build an interpolate satisfying the mass balance condition.

To understand this element better, we now try to look at its elementary vortices. We have here $3(n-1)^3 + 3 \times 3(n-1)^2 n = O(12\, n^3)$ degrees of freedom on an $n \times n \times n$ mesh, linked by $n^3 - 2$ linear constraints. This leaves $9(n-1)^3 + 3(n-1)^2 n - (n-2)^3$ independent vortices. To identify these vortices we consider a $2 \times 2 \times 2$ array on which 15 vortices must be found. In fact we can use the same device as we used in the preceding example: we consider a mid-plane slice of our $2 \times 2 \times 2$ array and we define on it the values of this velocity so that they correspond to one of the two-dimensional vortices of Figure 7. An example is shown in Figure 13.

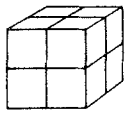

(a) 2×2×2 array

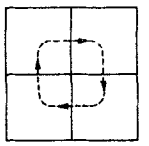

(b) A 2-D vortex on P vortex

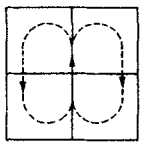

(c) A twin vortex on P

Figure 13

We thus make the vortices of Example 2 two elements thick. We thus found seven such vortices for each slice and we have three slices. However, the spurious vortices parallel to the edges are counted twice: we have found exactly the 15 predicted vortices. For larger arrays these vortices are not all linearly independent, $(n-2)^3$ can be expressed using the others.

As was the case for the analogous 2-D element the $3(n-1)^2n$ 'vortices' parallel to the edges are spurious: they do not represent a true recirculating flow. We shall try to eliminate them in our next example. But before doing this let us consider more complex flow fields. Vortices such as the one depicted in Figure 13(b) can be piled to yield a $2\times2\times k$ roll.

Summing two twin vortices [Figure 13(c)] in perpendicular planes yields a crude doughnut. We may conclude that the limit of resolution of this element is two-elements large.

Example 7: Restricted triquadratic velocity–constant pressure element (R_2-P_0)

The previously described element contains spurious vortices. The way to eliminate them is now clear: we can restrict our triquadratic velocity to have a linear tangential component along the edges. This can be done without loss of accuracy as, with constant pressure, we cannot expect better than first-order convergence.

The way to introduce such a restriction is the same as we used for the R_2-P_0 of Example 4. We choose, along an edge, an orthonormal system of three vectors, the first being tangential to the edge. We then *correct* a Q_1-P_0 element by adding, on each edge, two shape functions chosen so that their values at mid-edge points are proportional to the components of each of the nontangential vectors.

This eliminates the $3(n-1)^2n$ spurious vortices and leaves $3(n-1)^3+2\times3(n-1)^2n = O(9n^3)$ degrees of freedom linked by n^3-2 constraints. We are thus left with the $9(n-1)^3-(n-2)^3$ *non-spurious* vortices of the previous example.

It must be noted that this element still does not satisfy the B.B. condition. However, relative to the previous example, the d.o.f. have been reduced by 25 per cent with no loss in the shape of complex structures, such as rolls.

Example 8: *The 'enriched' trilinear velocity–constant pressure element* $(Q_1^+ - P_0)$

The three previously described elements lacked the essential control feature in order to satisfy the B.B. condition: a mid-face node. We now design a simple element on which this control does exist. We thus consider a Q_1 element to which we add a 'bubble' Q_2 function on *each face*. For instance, on the reference cube this bubble can be written for the $z = 1$ face:

$$b(x, y, z) = \tfrac{1}{2}(z+1)(x^2-1)(y^2-1). \tag{26}$$

This function vanishes on the other faces and its value is 1 at a mid-face point. As we need only $\mathbf{u}_h \cdot \mathbf{n}$ as a d.o.f. we shall again use the same trick: we take the values of a *correction* velocity at mid-face points proportional to the unit normal to the face. The use of a reference element is just an adaptation of the process described in Example 4.

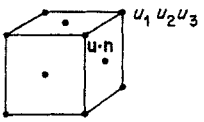

Figure 14. The $Q_1^+ - P_0$ element

Adding this extra nodal value on each face is enough to build the needed interpolate: this element satisfies the B.B. condition and is probably the simplest 3-D element to do so. This unfortunately does not mean that it is more accurate (at least on regular meshes). To see this we again try to find the elementary vortices.

On our $n \times n \times n$ array, we have $3(n-1)^3 + 3n^2(n-1) = O(6n^3)$ d.o.f. linked by $n^3 - 1$ linear constraints. We thus have $3(n-1)^3 + 3n^2(n-1) - (n-1)^3$ linearly independent vortices. These are no longer 2-D vortices with added thickness, they are really new. Let us consider a $2 \times 2 \times 2$ array on which eight vortices must be found. Figures 15 and 16 present the two basic ones from which all the others can be deduced by symmetry.

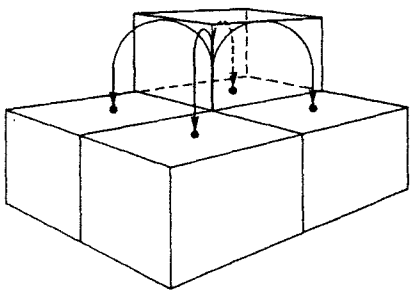

Figure 15

Figure 15 depicts what we could call a *fountain*, it consists of four vortices (we only show the upper half of them) moving up in parallel at the mid-vortex and recirculating through the adjacent faces.

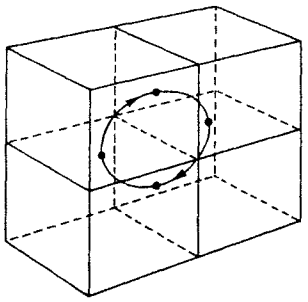

Figure 16

Figure 16 is simply a vortex turning around an edge. These vortices are at first glance analogous to the six vortices of Example 5 on a $3\times3\times3$ array.

There is one copy of the fountain of Figure 15 for each co-ordinate direction and one vortex around each edge of which only five are linearly independent. This leaves the expected number of eight. The trouble with this is that the vortices of Figure 16 *cannot* pile to form rolls: they cannot cross element boundaries. The smallest possible roll is in fact the $3\times3\times k$ one of Example 5.

It is rather hard to conclude anything from this, although the element satisfies the B.B. condition. It can therefore be used in a non-regular mesh without fear. The number of degrees of freedom is approximately double with respect to the Q_1-P_0 element and this is reflected by an increased number of vortices and a reduction of their size. However, there seems to be a *qualitative deficiency* of these vortices since they do not easily assemble into complex flows. Only numerical experiments can give the final answer. A possible way to escape from this dilemma is to use the following element.

Example 9: Enriched-restricted triquadratic velocity–constant pressure element ($R_2^+-P_0$)

Adding a bubble on the faces is the natural way to get elements satisfying the B.B. condition. As this process was not really satisfactory with the Q_1 element we now try to enrich the R_2-P_0 element of Example 7.

We therefore obtain an element where the tangential velocity is linear along edges and $\mathbf{u}\cdot\mathbf{n}$ has been added as a d.o.f at mid-face points.

We thus use u_1, u_2, u_3 at the vertices, u_a and u_b, which are two non-tangential components along edges, and $\mathbf{u}\cdot\mathbf{n}$ on faces (Figure 17).

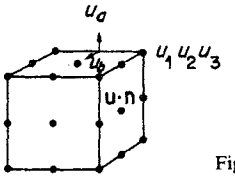

Figure 17

This element satisfies the B.B. condition. It contains as special cases the elements Q_1-P_0, $Q_1^+-P_0$, R_2-P_0 and it must be as rich in vortices as any of these.

We have on an $n\times n\times n$ mesh $2(n-1)^3+6n(n-1)^2+3n^2(n-1)=O(12n^3)$ d.o.f. and n^3-1 linear constraints. This makes $O(11n^3)$ independent vortices: all those we previously

described are there but of course they are not all independent. This element can make $2\times2\times k$ rolls and a quite good doughnut exists on a $2\times2\times2$ array. It is qualitatively the best of the elements considered so far.

Example 10: *Full triquadratic velocity–linear pressure element* $Q_2^{(27)}-P_1$

To make this analysis complete and to consider the analogue of the full 2-D biquadratic velocity–constant pressure element, we consider the simplest element which is second-order accurate and satisfies the B.B. condition. We approximate velocity by a complete 27-node triquadratic element and we consider, on each element, a linear pressure. As it was already the case in two dimensions we can eliminate the internal velocity nodes by the three non-constant components of pressure. This results in a 26-node element in each velocity component and a constant pressure. We have $3(n-1)^3+9n(n-1)^2+9n^2(n-1)=O(21n^3)$ d.o.f. and (n^3-1) constraints. On a $2\times2\times2$ array this yields 50 linearly independent vortices. They can easily be identified: we add to those already found the six spurious vortices of Example 6 which are now genuine recirculating flows and we add 24 twin vortices acting on two adjacent elements (Figure 18), generated by the d.o.f. tangential to the faces.

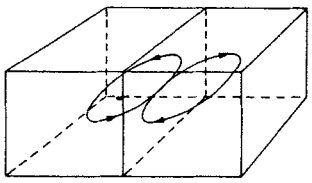

Figure 18

This may help in the precision of small structures but the size of the smallest rolls *is not reduced.* It is then questionable whether this element is worth its cost.

A summary of these results is given in Table II.

What should one conclude? The answer is different whether one cares or not about spurious pressure modes and this should be related to the kind of mesh used: spurious modes

Table II

Element	Approximate number of d.o.f.	Approximate number of independent vortices	Order of accuracy	Remarks
Q_1-P_0	$3n^3$	$2n^3$	$O(h)$	$3n-2$ spurious pressure modes
$Q_1^+-P_0$	$6n^3$	$5n^3$	$O(h)$	B.B. satisfied
$Q_2^{(20)}-P_0$	$12n^3$	$11n^3$	$O(h)$	1 spurious checkerboard pressure mode and spurious vortices
R_2-P_0	$9n^3$	$8n^3$	$O(h)$	Spurious vortices have been eliminated
$R_2^+-P_0$	$12n^3$	$11n^3$	$O(h)$	B.B. condition satisfied
Q_2-P_1	$21n^3$	$20n^3$	$O(h^2)$	Internal nodes are eliminated

can be filtered out on regular meshes but become impure (Sani *et al.*[1]) on non-regular meshes and are a potential hazard. For a regular mesh we recommend the use of the $R_2 - P_0$ element. The analysis we presented shows that it can perform as well as, or better on a 2^3 array than the $Q_1 - P_0$ element with a 3^3 array. Thus we compare

$$q \times (\tfrac{2}{3})^3 n^3 = \tfrac{8}{3} n^3$$

to $3n^3$ d.o.f. and the count is clearly in favour of $R_2 - P_0$. If one wants to have a really safe element satisfying the B.B. condition the point is less clear. Second-order accuracy seems to be very expensive. The choice is between $Q_1^+ - P_0$ and $R_2^+ - P_0$.

Using $Q_1^+ - P_0$ doubles the number of d.o.f. and is not a *clear* advantage with respect to accuracy although there is surely some gain. However, we cannot claim doing as well with $\hat{n} = \frac{2}{3} n$ as we did before. If we move to $R_2^+ - P_0$ then the claim $\hat{n} = \frac{2}{3} n$ is more than justified and we compare

$$12 \times (\tfrac{2}{3})^3 n^3$$

to $3n^3$ or $3{\cdot}56n^3$ to $3n^3$. This is a 20 per cent increase in the number of d.o.f. The gain in precision is probably sufficient to justify this. Anyhow $R_2^+ - P_0$ is surely preferable to the classical $Q_2^{(20)} - P_0$. As to $Q_2^{(20)} - P_1$ elements not discussed here, it is clear that they are to be avoided as such: just add an internal velocity mode and use it to eliminate the non-constant component of pressure and you fall back on an improved $Q_2^{(20)} - P_0$ element, which might claim second-order accuracy but does not satisfy the B.B. condition. To get the B.B. condition we should add a $\mathbf{u}_n \cdot \mathbf{n}$ node at mid-face points and this would yield $O(15n^3)$ degrees of freedom.

CONCLUSION

We have tried to compare various elements on the basis of their ability to represent incompressible flow fields. We tried not to give proof but to present a qualitative point of view on the behaviour of elements. We hope this will be of some use for the people involved in actual computations who want to make the best choice for their needs. We have presented some new elements and we have shown them to be competitive with more standard choices.

REFERENCES

1. R. Sani, P. Gresho, R. Lee, D. Griffiths and M. Engelman, 'The cause and cure (?) of the spurious pressures generated by certain FEM solutions of the incompressible Navier–Stokes equations', Parts 1 and 2 of *Int. j. numer. methods fluids*, **1,** 17–43 and **1,** 171–204 (1981), respectively.
2. D. Malkus and T. Hugues, *Comp. Meth. Appl. Mech. and Eng.*, **15,** 63 (1978).
3. R. Temam. *Navier–Stokes Equations*, North-Holland, Amsterdam, 1977.
4. V. Girault and P. A. Raviart, *Finite Element Approximations of the Navier–Stokes Equations*, Springer Verlag: *Lecture Notes in Mathematics* 749 (1979).
5. M. Fortin, 'An analysis of the convergence of mixed finite element methods', *RAIRO Anal. Num.*, **11,** R–3, 341–354 (1977).
6. M. Crouzeix and P. A. Raviart, 'Conforming and non-conforming finite element methods for solving the stationary Stokes equations, *RAIRO, Anal. Num.*, **7,** R3, 33–76 (1973).
7. M. Fortin, 'Utilisation de la méthode des éléments finis en mécanique des fluides', *Calculo*, **XII,** 405–441 (1975).
8. F. Brezzi, 'On the existence, uniqueness and approximation of saddle point problems arising from Langrangian multipliers', *RAIRO, Anal. Num.*, **8**, R2, 129–151 (1974).
9. I. Babŭska, 'Error bounds for finite element method', *Numer. Math*, **16,** 322–333 (1971).
10. D. F. Griffiths, 'The construction of approximately divergence-free finite elements', in *Mathematics of Finite elements and Applications* (Ed. J. R. Whiteman), Academic Press, 1979.
11. D. F. Griffiths, 'Finite elements for incompressible flow', *Math. Meth. in Appl. Sci.* **1,** 16–31 (1979).
12. G. Strang and G. Fix, *An analysis of the finite element method*, Prentice-Hall, Englewood Cliffs, N.J., 1973.